

Supporting Material

Cyclic N-terminal loop of amylin forms non-amyloid fibers

Stephanie M. Cope,^{§¶} Sandip Shinde,[‡] Robert B. Best^{#†}, Giovanna Ghirlanda,[‡] and Sara M. Vaiana^{*§¶}

[§]Center for Biological Physics, [¶]Department of Physics, [‡]Department of Chemistry and Biochemistry, Arizona State University, Tempe 85287, USA. [#]Department of Chemistry, Lensfield Road, Cambridge, CB2 1EW, United Kingdom. [†]Laboratory of Chemical Physics, National Institute of Diabetes and Digestive and Kidney Diseases, National Institutes of Health, Bethesda, Maryland 20892-0520, U.S.A..

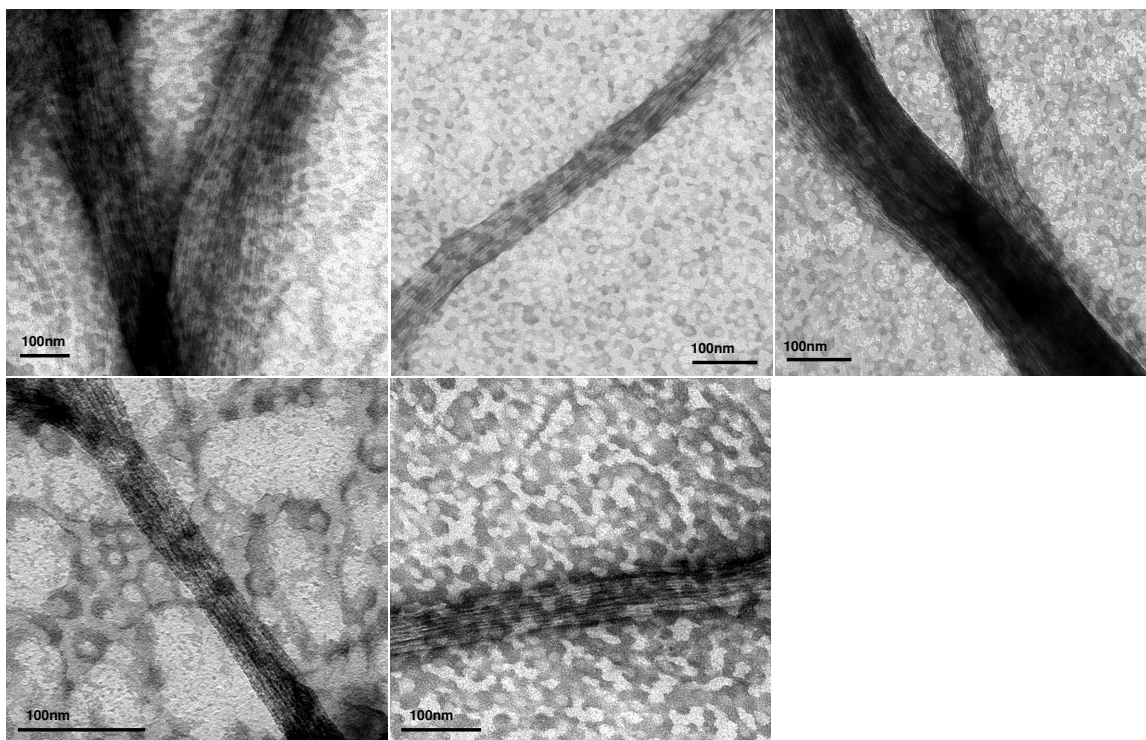


Figure S1. TEM images of N_loop fibers formed at different peptide concentrations. From top left to bottom right: 50mM, 1.4mM, 1mM, 0.15mM, 57μM. All scale bars are 100nm. Lyophilized peptide was dissolved in 50mM NaAc, pH=4.9. Samples were deposited onto grids within 1 hour of sample preparation. Fibers are evident at concentrations as low as 57μM.

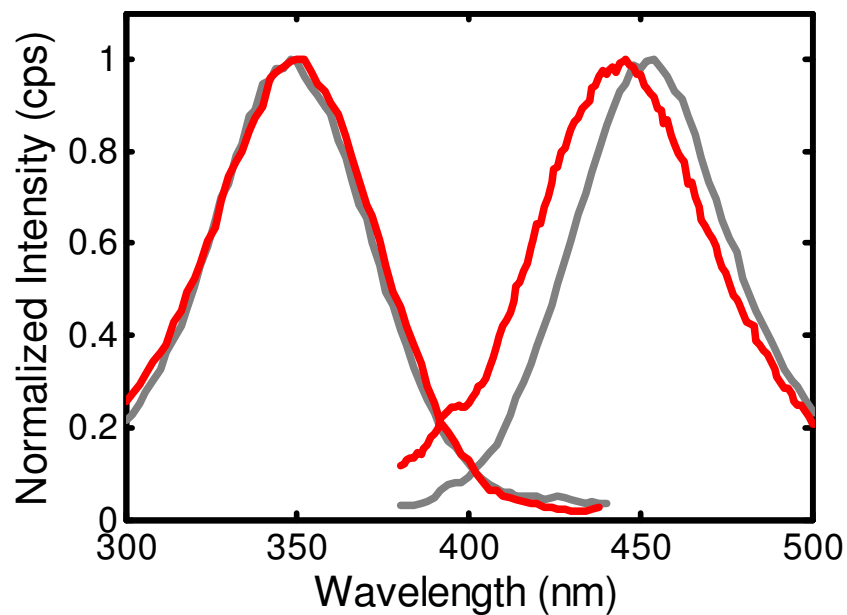


Figure S2. Thioflavin T binding assay of N_loop fibers. Fluorescence excitation ($\lambda_{em}=450\text{nm}$) and emission spectra ($\lambda_{ex}=350\text{nm}$) of 10 μM ThT solutions in 50mM NaAc pH=4.9, in the absence (red) and presence (grey) of 12.5mM N_loop fibers. Only a slight shift in the emission spectrum of ThT was detected, in contrast to the large shift of emission and excitation peaks ($\lambda_{ex} =450\text{nm}$ and $\lambda_{em}=480\text{nm}$) typically observed in the presence of amyloid fibers.

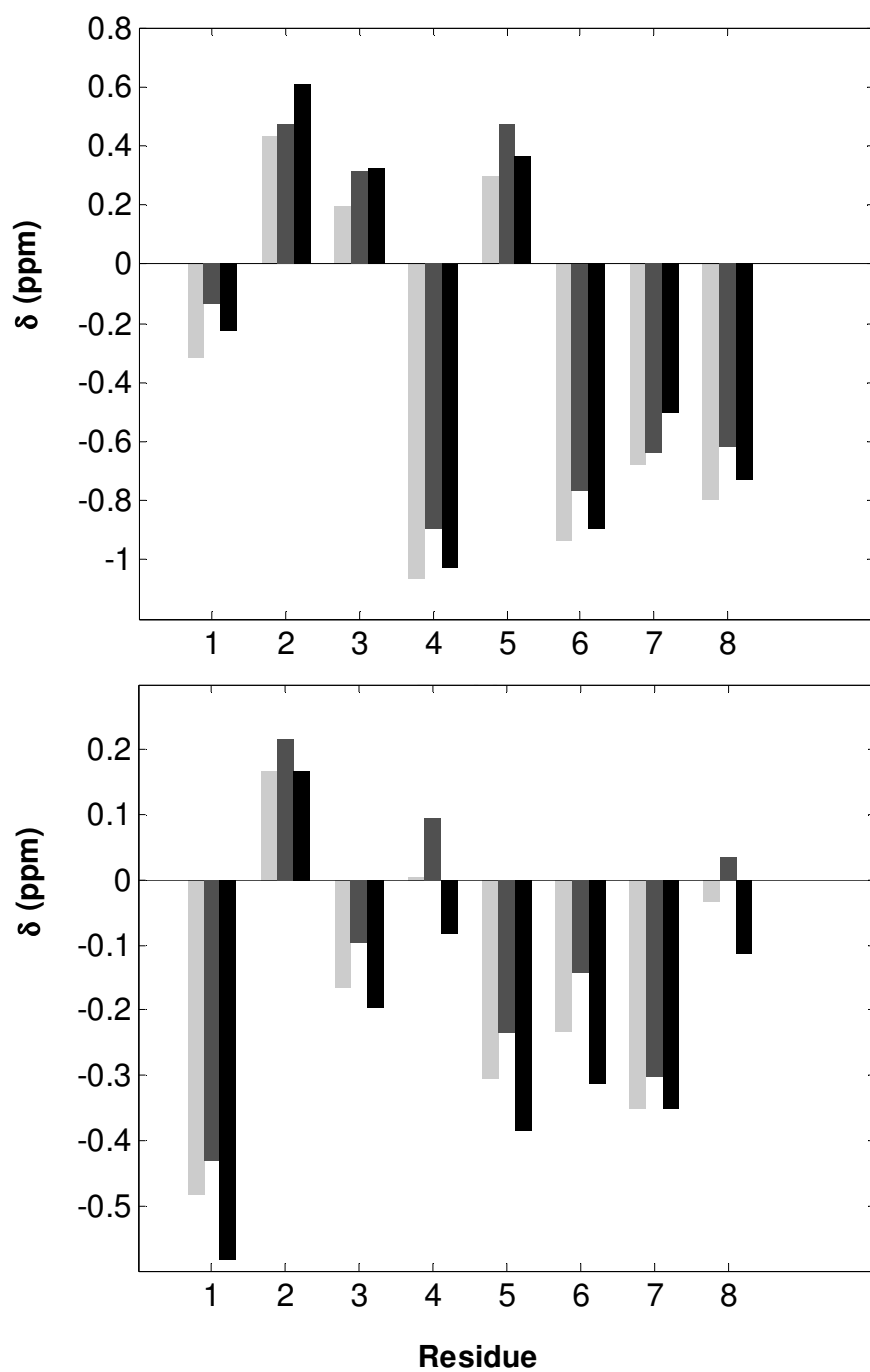


Figure S3. $^1\text{H}^{\text{N}}$ (top) and $^1\text{H}^{\alpha}$ (bottom) secondary chemical shifts for N_loop, calculated using reference random coil chemical shifts from different libraries: Kjaergaard and Poulsen (light gray), Tamiola et al. (dark gray), and De Simone et al. (black).

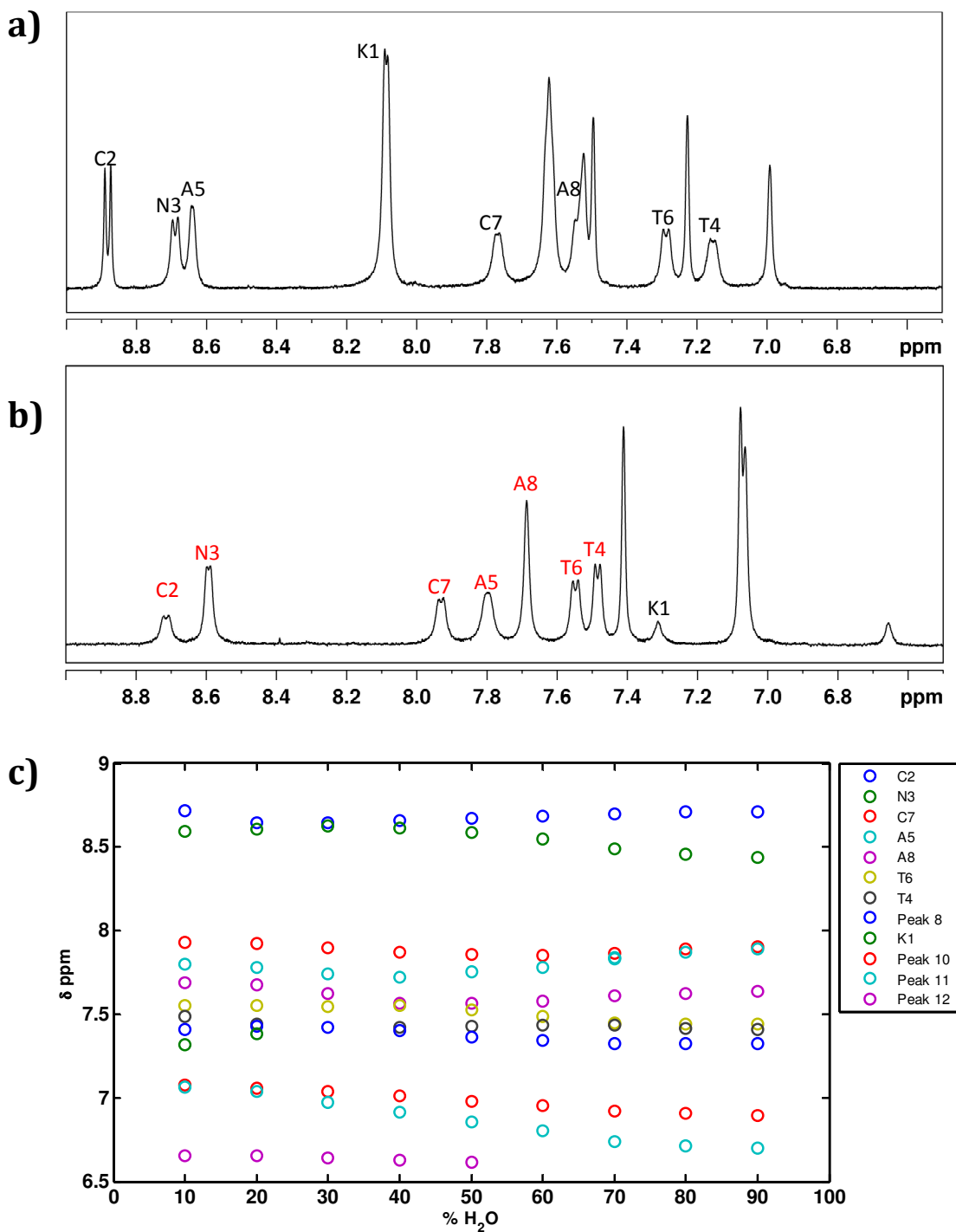


Figure S4. To investigate the effect of solvent on N_loop structure we obtained ¹H-1D NMR spectra of N_loop in 90%, 80%, 70%, 60%, 50%, 40%, 30%, 20% and 10% DMSO by directly diluting a 100%DMSO, 1.3 mM peptide sample in non-deuterated buffer (50mM NaAc pH=4.9, prepared with H₂O and deuterated salts/acid). (a) 100% DMSO spectrum (b) 90% DMSO spectrum. (c) peak positions as a function of dilution, from 90%DMSO to 10%DMSO. As expected, an evident change in spectrum occurs between the

100% and 90% DMSO samples, reflecting the change from aprotic to protic solvent conditions (a,b). By contrast, the peak positions hardly change after further dilutions, all the way down to 10% DMSO (c). The 90% DMSO peaks labeled in red (b) were assigned by assuming that each doublet/singlet shifted minimally respect to the 100%DMSO spectrum. This was based on the observed differences in chemical shifts between our 100% DMSO sample and those of both Yonemoto et al. and Williamson et al. in buffer (Figure 4). The K1 peak was assigned directly from TOCSY analysis of the 90% DMSO spectrum. All spectra were acquired at 25°C on a 500 MHz Varian spectrometer. Presaturation was used to suppress water in all measurements containing H₂O. Comparison between secondary chemical shifts obtained here and those shown in Figure 4 are shown in Figure S5.

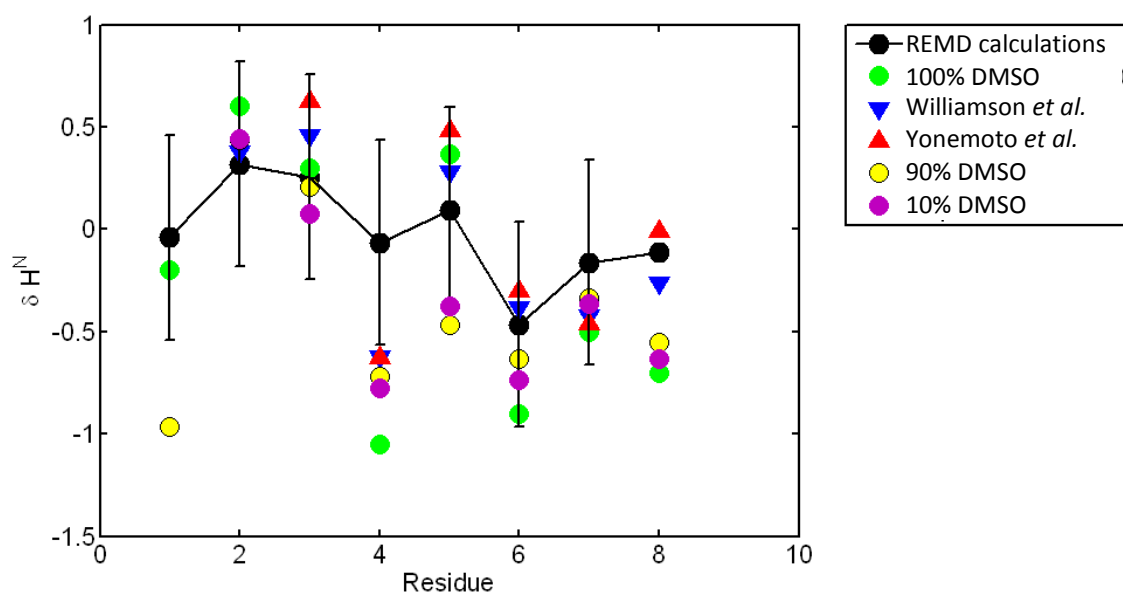


Figure S5 Comparison between secondary chemical shifts for N_loop in 100% DMSO (Figure 4 main text) and in 90% and 10% DMSO (obtained from 1D NMR of Figure S7). Apart from K1, which changes protonation state in water versus DMSO and is absent in the previous publications (due to proton exchange with the solvent), the observed chemical shifts do not show significant changes from DMSO to water-like solvent. This supports the conclusion that the DMSO has very little effect on the structure of the N_loop and that this structure is maintained in full length IAPP.

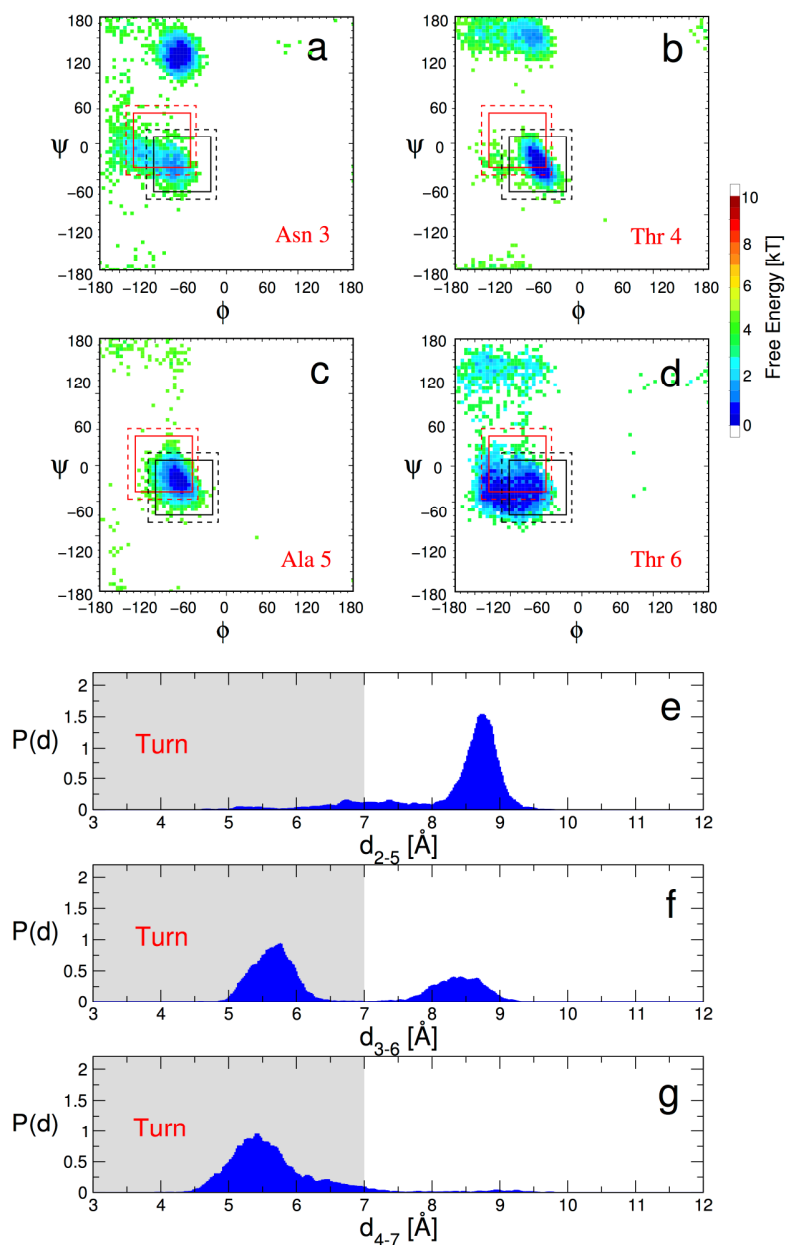


Figure S6. Geometric criteria for type I turn formation in N_loop: (a-d) Ramachandran maps of interior residues of N_loop. For a type I β -turn from residues i to $i+3$, the allowed Ramachandran angles of residues $i+1$ and $i+2$ are shown by black and red boxes respectively. Solid and broken lines indicate a range of 40 or 50 degrees respectively, with respect to the ideal turn angles(1). (e-g) Distance between alpha carbon atoms of residues $i, i+3$ for different i ; this distance should be less than 7 Angstroms for a turn to be defined. Based on these geometric criteria, a type I β -turn is present at residues 3-6 most of the time, with a significant fraction of type I turn also present at residues 4-7. The criteria for a type II turn, for which the ideal Ramachandran angles are i : $(-60, 120)$; $i+1$: $(80, 0)$, are clearly not satisfied.

1. Hutchinson, E. G., and J. M. Thornton. 1994. A Revised Set of Potentials for Beta-Turn Formation in Proteins. *Protein Science* 3:2207-2216.

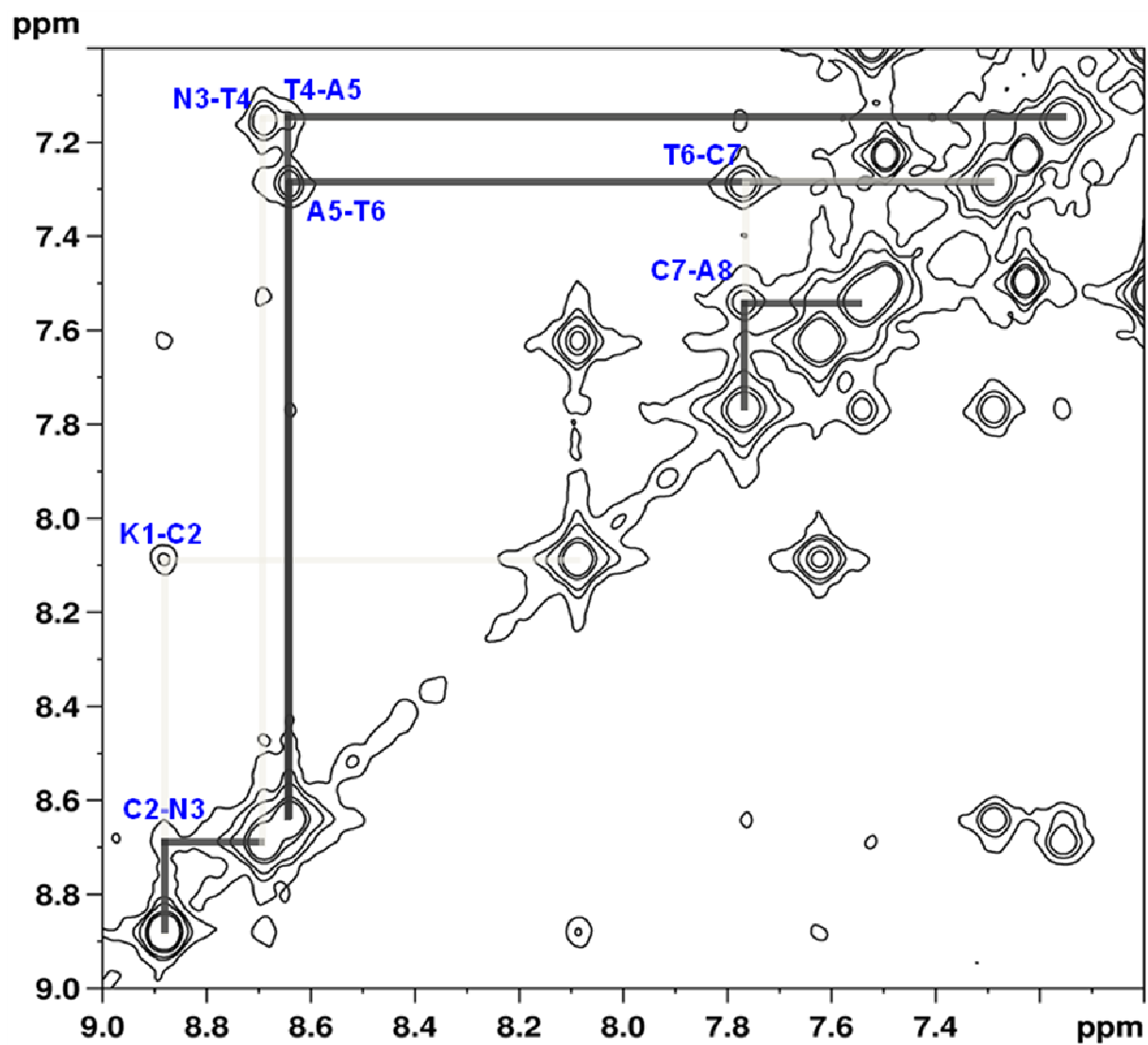


Figure S7. NMR spectrum of $i \rightarrow i+1$ in NH-NH region (400 ms NOESY)

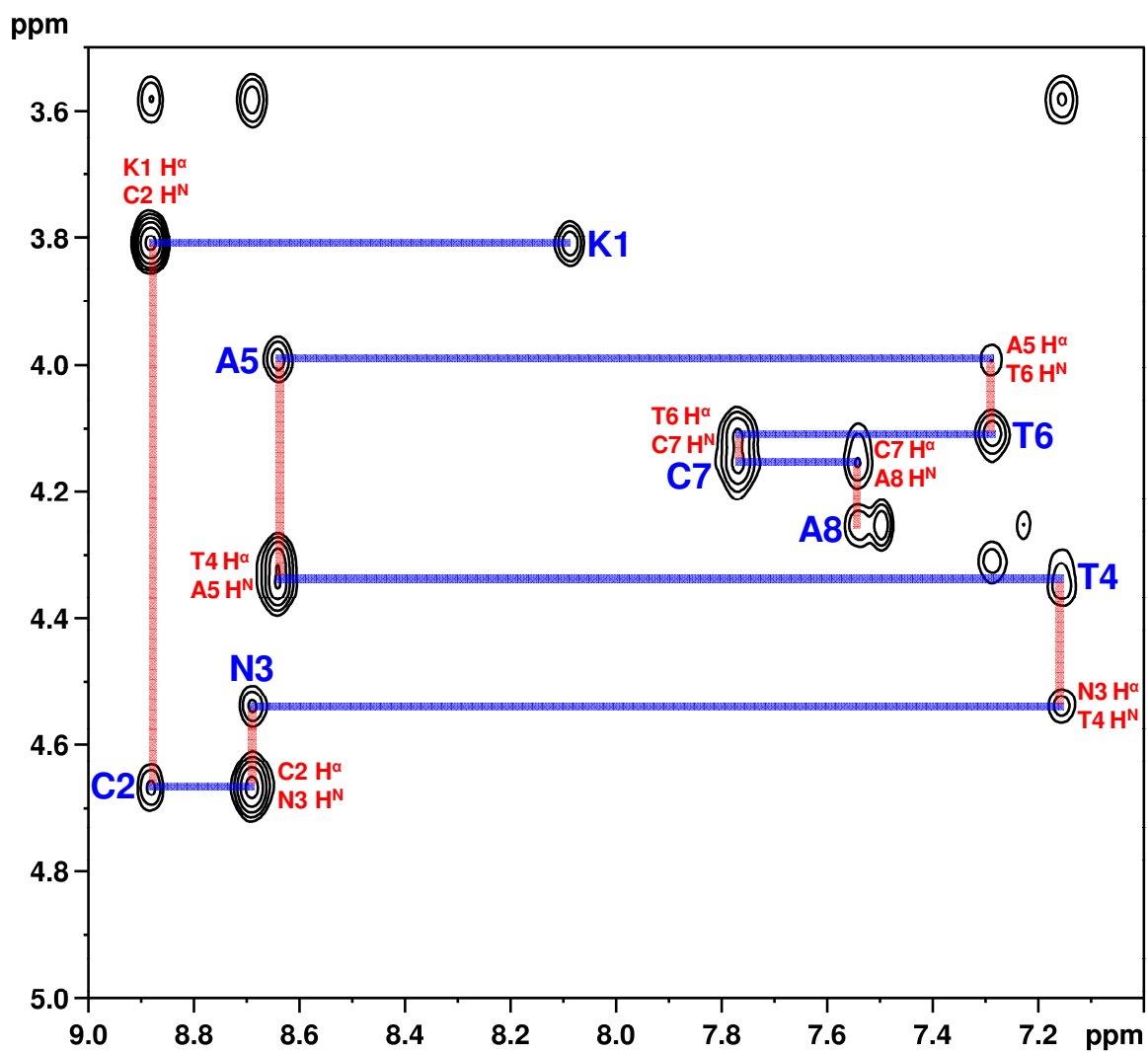


Figure S8. Backbone walk (400 ms NOESY)

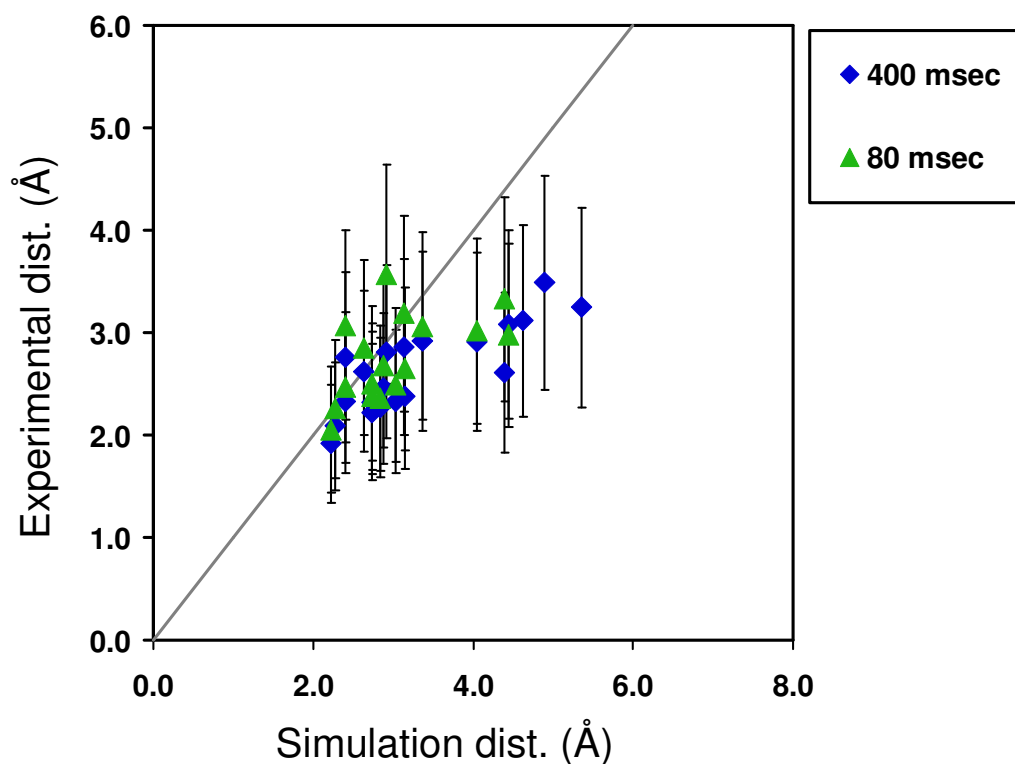


Figure S9. Distances estimated from NOE peak intensities of all assignable crosspeaks visible in NOESY spectrum, compared to average distances obtained from REMD simulations. The straight line corresponds to $y(x)=x$. There is a good correlation between the NOEs reported and the average MD distances. The quantitative agreement is lost at larger distances, most likely because of spin diffusion effects.

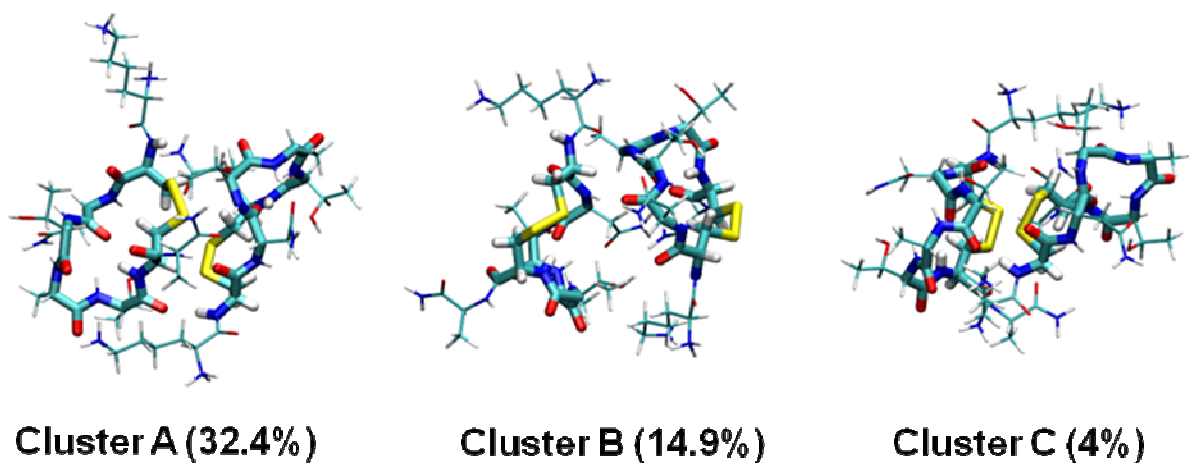


Figure S10. Major clusters (of associated states) populated by the N_loop dimer in 298 K replica of REMD simulations.

Table S1. $^1\text{H}^{\text{N}}$ and $^1\text{H}^{\alpha}$ Chemical Shifts for N_loop in 100% DMSO

K1	N 8.086	α 3.808
C2	N 8.881	α 4.667
N3	N 8.687	α 4.534
T4	N 7.152	α 4.346
A5	N 8.636	α 3.985
T6	N 7.285	α 4.107
C7	N 7.768	α 4.148
A8	N 7.54	α 4.255